A Compliance Control Strategy for Robot Manipulators Under Unknown Environment

Byoung-Ho Kim*
School of Electrical Engineering and Computer Science, Hanyang University
Sang-Rok Oh
Intelligent System Control Research Center, KIST
Il Hong Suh, Byung-Ju Yi
School of Electrieal Engineering and Computer Science, Hanyang University

In this paper, a compliance control strategy for robot manipulators that employs a self-adjusting stiffiness function is proposed. Based on the contact force, each entry of the diagonal stiffness matrix corresponding to a task coordinate in the operational space is adaptively adjusted during contact along the corresponding axis. The proposed method can be used for both the unconstrained and constrained motions without any switching mechanism which often causes undesirable instability and/or vibrational motion of the end-effector. The experimental results involving a two-link direct drive manipulator interacting with an unknown environment demonstrates the effectiveness of the proposed method.

Key Words : Robot Manipulator, Compliance Control, Self-Adjusting Stiffness Function

1. Introduction

When a robot manipulator is applied to work environments such as performing service tasks and industrial operations, manipulation tasks often require a series of contact operations. A contact motion is typically obtained by phase transition from an unconstrained mode to a constrained mode. However, during the transition period, the system often experiences unstable behaviour such as bouncing back and forth due to a switching of the control mode from the unconstrained mode to the constrained mode, or vice versa. In fact, a conventional position servo for an industrial robot is designed to be infinitely stiff which is appropriate when the manipulator is applied to follow a given trajectory in the free space, and hence it will reject all force disturbances acting on the system. However, once a contact is made between the end-effector and the environment, high stiffness of the end-effector or the environment may cause the manipulator to fail to maintain the contact. Small variations in relative positions due to either inaccurate position information or errors in position servo can produce excessive contact forces. To remedy this problem, a force servo instead of a position servo may be used. An ideal force servo exhibits zero stiffness and is able to maintain the desired force. However, the force servo cannot be useful for trajectory following due to sensitive positional variations even for small external force distubances. One way to alleviate this problem is to use a compliant motion controller : Some axes of the task coordinate are selected to be force controlled, and the others to be position-controlled.

In order to handle the interaction of a robot manipulator with the environment, many research works have been reported in the field of the compliant motion control of robot manipulators

* Corresponding Author,
E-mail : kbh@incorl.hanyang.ac.kr
TEL : +82-31-408-5802 ; **FAX** : +82-31-408-5803
School of Electrical Engineering and Computer Science, Hanyang University, and Intelligent System Control Research Center, KIST, 1271 Sa-1dong, Ansan Gyunggi-do 425-791, Korea, (Manuscript **Received** January 11, 2000 ; **Revised** June 21, 2000)

(Kim, 1999 ; Kang, 1998 ; Schutter, et al., 1988 ; Vukobratovič, 1994). The well known hybrid position/force control approach (Raibert, et al., 1981 ; Yoshikawa, 1987) is based on an orthogonal decomposition of the task space. In the scheme, however, since the selection matrix should be determined a *priori* to denote either the position controlled or force controlled axis, it can not be used for tasks that interact with an unknown environment. A stiffness adaptation scheme (Oh, et al., 1995) based on the position error has been proposed. However, since the exact trajectory tracking is assumed with high stiffiness gains in the unconstrained space, a recovery mechanism which resets the stiffness adaptation procedure caused by any unexpected position error in the unconstrained space should be taken into consideration. Also, a parallel control scheme (Chiaverini, et al., 1998) with stiffness adaptation has been proposed. The method is useful for regulating the contact force in the constrained space. But, since it also does not have a recovery procedure in the stiffness adaptation algorithm, the trajectory tracking performance can not be guaranteed when the task space is changed from the constrained space to the unconstrained space after the constrained task is completed.

In order to handle a contact control problem in an unknown environment, a novel type of compliant contact control method is proposed in this paper. Specifically, the stiffness of the end-effector of a robot manipulator is automatically adjusted based on the contact force with its environment without any switching between the constrained and unconstrained spaces, and hence the method has a stiffness adaptatioin capability for a successful motion control of the robot manipulator in both the constrained and unconstrained spaces. The proposed compliance control algorithm can be effectively applied to cooperative motion control, soft touching and grasping by robot hand.

2. Compliance Control Method with Adaptive Stiffness Function

2.1 Adaptive stiffness function

When an n degrees-of-freedom robot manipulator makes contacts with the environment, the robot or the environment will deform and a reaction force at the end-effector will be transmitted into each joint. If f denotes the reaction force vector at the end-effector in the operational coordinate, then the dynamic equation takes the following form (Lewis, et al., 1993),

$$\tau = M(q)\,\ddot{q} + H(q,\,\dot{q})\,\dot{q} + g(q) + J^T(q) f \tag{1}$$

where q, $\dot{q}$, and $\ddot{q}$ are $n\times 1$ vectors of joint positions, velocities, and accelerations, respectively. τ is the $n\times 1$ vector of joint torques supplied by the actuator. $M(q)$ is the $n\times n$ symmetric positive definite inertia matrix and $H(q,\,\dot{q})$ is the $n\times n$ structural matrix of centripetal and Coriolis forces. $g(q)$ is the $n\times 1$ gravity vector and $J(q)$ is the $n\times n$ Jacobian matrix relating joint velocities to task space velocities.

In robotic applications, the position servo gains should be stiff enough to be able to follow the desired trajectory in the unconstrained space. Also, generation of undesirably large contact forces should be avoided by adjusting the stiffness gains of the end-effector in the constrained space. To accomplish these objectives, we propose a compliance control method that uses self-adjusting stiffness function based on the contact force.

In this paper, the control input for a compliant contact control of a robot manipulator is given by

$$\tau = K_q(f)\,(q_d - q) - K_d(f)\,\dot{q} + g(q) \tag{2}$$

in the joint space, where q_d is $n\times 1$ vector of desired joint positions. $K_q(f)$ is the position feedback gain matrix and $K_d(f)$ is the velocity feedback gain matrix in the joint space. From the basic stiffness formulation in Salisbury's work (Salisbury, 1980), the joint stiffness matrix $K_q(f)$ is given by

$$K_q(f) = J^T K_c(f) J \tag{3}$$

where $K_c(f)$ denotes a desired $n\times n$ stiffness

matrix in the operational space.

By using Eq. (3), we can rewrite Eq. (2) as follows

$$\tau = J^T(q)\,(K_c(f)\,(x_d - x) - K_v(f)\,\dot{x}) + g(q) \tag{4}$$

where x, $\dot{x}$, and x_d are the $n \times 1$ position, velocity, and desired position vectors in the operational space, respectively. $K_v(f)$ denotes $n \times n$ damping matrix in the operational space.

In Salisbury's work (Salisbury, 1980), the stiffness in the operational space is controlled by controlling the joint stiffness corresponding to that in the operational space by using the stiffness mapping described by Eq. (3), where it is assumed that the desired operational stiffness characteristic is exactly known. This assumptioin is quite restraining and also may not be available in the real work environment. In the hybrid position/force control method (Raibert, et al., 1981 ; Yoshikawa, 1987), a position control or force control method is independently developed, and then the position control or force control is selected by using a *priori* determined selection matrix accoriding to the position controlled or force controlled axis, where it is assumed that the positioin controlled or force controlled axis is exactly known. Those methods have some problems as follows. First, since the work space of the industrial robots employed in factories is well-structured, it is safe to assume that the work space is previously known. But because we can not exactly know the work space due to existing uncertainty for service robots, it is not easy to determine the desired stiffness gains in the operational space and the selection matrix by considering the external environment a *priori*. Second, the hybrid position/force control method is theoretically applicable. But since the switching mechanism often causes undesirable instability and/or vibrational motion of the end-effector due to sensor noise, time delay, or dynamic characteristics of the robotic system, the method may not be easy to apply in practical situations. In practical robotic applications, it is very important to reduce the task time through fast trajectory following in the unconstrained space, but a dextrous motion control is important in the constrained space. In general, high stiffness servo gains are required for fast trajectory following in the unconstrained space, but low stiffness servo gains are required for achieving a compliant contact in the constrained space. Therefore, these two objectives should be simultaneously considered in real systems.

In order to handle these problems, an adaptive stiffness function is also proposed in this paper as follows. For convenient representation, the proposed adaptive stiffness function is described in three-dimensional space.

From Eqs. (2) and (4),

$$K_q(f) = J^T K_c(f) J,\ K_d(f) = J^T K_v(f) J \tag{5}$$

where

$$K_c(f) = \begin{pmatrix} K_{cx}\exp(-s_x|f_x|) & 0 & 0 \\ 0 & K_{cy}\exp(-s_y|f_y|) & 0 \\ 0 & 0 & K_{cz}\exp(-s_z|f_z|) \end{pmatrix} \tag{6}$$

and

$$K_v(f) = \begin{pmatrix} \alpha_x & 0 & 0 \\ 0 & \alpha_y & 0 \\ 0 & 0 & \alpha_z \end{pmatrix} K_c(f) \tag{7}$$

In Eq. (6), $\exp(\cdot)$ denotes an exponential function, and K_{cx}, K_{cy}, and K_{cz} represent x, y, and z-directional operational stiffness gains, respectively. These stiffness gain parameters are chosen to be positive constants such that the asymptotic stability is ensured in the unconstrained space. The slope parameters s_x, s_y, and s_z are selected to be positive values and play the role of determining the rate of decrease. f_x, f_y, and f_z are the directional contact forces sensed at the end-effector. $|\cdot|$ means the absolute value. It is assumed that the effect of the coupling stiffness elements is negligible. In Eq. (7), α_x, α_y, and α_z are positive scalar scaling coefficients.

Several points can be discussed about the proposed adaptive stiffness conrol method. First, when a robot manipulator is working in the unconstrained space, the contact force for each direction of the end-effector is not generated and hence $f_x = f_y = f_z = 0$ and $\exp(\cdot) = 1$. Thus, initially selected high stiffness gains K_{cx}, K_{cy}, and

K_{cz} that satisfy the fast tracking performance in the unconstrained space can be applied without changing of the stiffness gains. In the constrained space, the stiffness gains of the end-effector decrease exponentially during the contact only along the corresponding axes. Consequently, the proposed method has the capability of self-adjusting the stiffness values appropriate for the given tasks regardless of whether the operation takes place in the constrained space or the unconstrained space. Second, since the stiffness gains of the end-effector are initially determined by considering all directions of the task space, it can be applicable to the industrial robot performing a pre-defined task, and because the stiffness gains can be adaptively controlled through an adaptive exponential function, it can be applied to service robots with no pre-defined work space. Third, the proposed method does not consider whether the task space is the unconstrained space or not, but considers whether the contact force of the end-effector exists or not. In other words, since the proposed method has no switching mechanism, it can be effectively used for both the unconstrained and constrained motion control and also it can be applied to problems soft contact and grasping by robotic hands.

2.2 Stability analysis

Now, we perform the stability analysis for the robot manipulator interating with an unknown environment by using the proposed stiffness adaptation strategy. The force exerted on the environment is defined by

$$f=K_w(x-x_w) \tag{8}$$

where K_w is an $n\times n$ diagonal, positive semi-definite, constant matrix that denotes the environmental stiffness, and x_w is an $n\times 1$ position vector measured in the task space for denoting the static location of the environment while x is the actual position vector of the end-effector.

Note that if the manipulator is not constrained in a particular task space direction, the corresponding diagonal element of the matrix K_w is assumed to be zero. Also, the surface friction is assumed negligible.

When the end-effector stiffness is adaptively changed by the proposed method in the constrained space, the stiffness $K_c(f)$ is replaced as in Eq. (6). Using from Eqs. (4) to (7), the closed-loop dynamics yield

$$M(q)\ddot{q}+H(q,\dot{q})\dot{q}=J^T(q)(K_c(f)\tilde{x} -K_v(f)\dot{x}-K_w(x-x_w)) \tag{9}$$

where $\tilde{x}$ is defined as positional tracking errors, x_d-x, in the task space.

To analyze the stability of the system, we utilize a Lyapunov-like function given by

$$V=\frac{1}{2}\dot{q}^TM(q)\dot{q}+\frac{1}{2}\tilde{x}^TK_c(f)\tilde{x} +\frac{1}{2}(x-x_w)^TK_w(x-x_w) \tag{10}$$

Differentiating Eq. (10) with respect to time and utilizing the Jacobian relation, $\dot{x}=J(q)\dot{q}$, we obtain

$$\dot{V}=\frac{1}{2}\dot{q}^T\dot{M}(q)\dot{q}+\dot{q}^TM(q)\ddot{q} +\frac{1}{2}\tilde{x}^T\dot{K}_c(f)\tilde{x}-\dot{q}^TJ^T(q)K_c(f)\tilde{x} +\dot{q}^TJ^T(q)K_w(x-x_w) \tag{11}$$

Substituting Eq. (9) into Eq. (11) and utilizing Jacobian relatioin yields

$$\dot{V}=\dot{q}^T\left(\frac{1}{2}\dot{M}(q)-H(q,\dot{q})\right)\dot{q} -\dot{q}^TJ^T(q)K_v(f)J(q)\dot{q}+\frac{1}{2}\tilde{x}^T\dot{K}_c(f)\tilde{x} \tag{12}$$

Applying the following skew-symmetric property(Lewis, et al., 1993) to Eq. (12),

$$\frac{1}{2}\dot{M}(q)-H(q,\dot{q})=0$$

and also utilizing Eq. (7) and the Jacotian relation, we have

$$\dot{V}=-\dot{x}^T\begin{pmatrix}\alpha_x & 0 & 0\\ 0 & \alpha_y & 0\\ 0 & 0 & \alpha_z\end{pmatrix}K_c(f)\dot{x}+\frac{1}{2}\tilde{x}^T\dot{K}_c(f)\tilde{x} \tag{13}$$

where $x=[x_x\ x_y\ x_z]^T$, $\tilde{x}=[\tilde{x}_x\ \tilde{x}_y\ \tilde{x}_z]^T$ in three-dimensional space.

After rearranging Eq. (13), and applying the condition $\dot{V}<0$, the following inequality equations can be constructed :

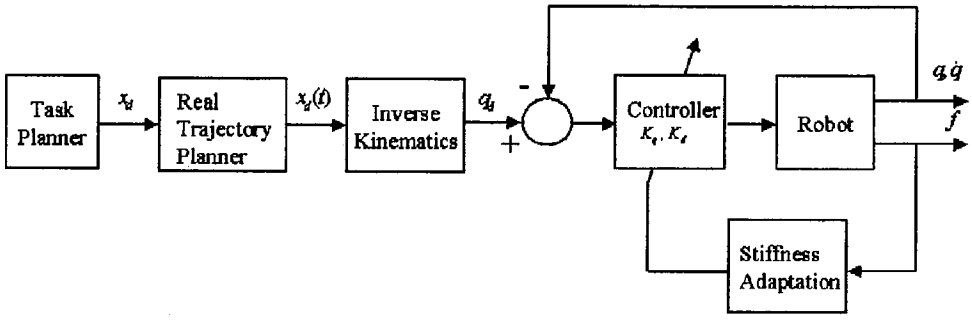

Fig. 1 The block diagram for compliant contact control

$$2\alpha_x \dot{x}_x^2 + \tilde{x}_x^2 s_x \dot{f}_x > 0 \tag{14}$$

$$2\alpha_y \dot{x}_y^2 + \tilde{x}_y^2 s_y \dot{f}_y > 0 \tag{15}$$

and

$$2\alpha_z \dot{x}_z^2 + \tilde{x}_z^2 s_z \dot{f}_z > 0 \tag{16}$$

In Eqs. (14), (15), and (16), the following sufficient conditions for stability can be obtained :

$$0 \le s_x < \frac{2\alpha_x \dot{x}_x^2}{\tilde{x}_x^2 |\dot{f}_x|} \tag{17}$$

$$0 \le s_y < \frac{2\alpha_y \dot{x}_y^2}{\tilde{x}_y^2 |\dot{f}_y|} \tag{18}$$

and

$$0 \le s_z < \frac{2\alpha_z \dot{x}_z^2}{\tilde{x}_z^2 |\dot{f}_z|} \tag{19}$$

Therefore, for small velocities, and large force variations, α_x, α_y, and α_z are chosen to be sufficiently large in such a way that s_x, s_y, and s_z could have reasonable positive values. The slope parameters ideally can be chosen as the maximum value satisfying the sufficient conditions. But, if the slope parameters are set to be near the boundary conditions for stable contact tasks, the system can easily become unstable due to external disturbances and therefore these parameters should be carefully chosen with the stability conditions in mind. On the other hand, if each slope is chosen to be zero, the proposed method is the same as the conventional active stiffness control method.

3. Implementation and Experimental Results

3.1 Implementation and experimental setup

In Fig. 1, the block diagram for the proposed compliance control method is shown. As shown in Fig. 1, the task planner initiates a surface tracking manipulation task that aims to achieve the following two subgoals simultaneously :

1) minimum variance path following and

2) regulation of a contact force of the axes of the end-effector orthogonal to the position or velocity controlled axes for path following.

The desired motion are not here specified as fixed functions of time. Instead, they are specified as functions of task-related motion quantities. In addition, a virtual desired path to be followed is intentionally given to be inside of the surface of

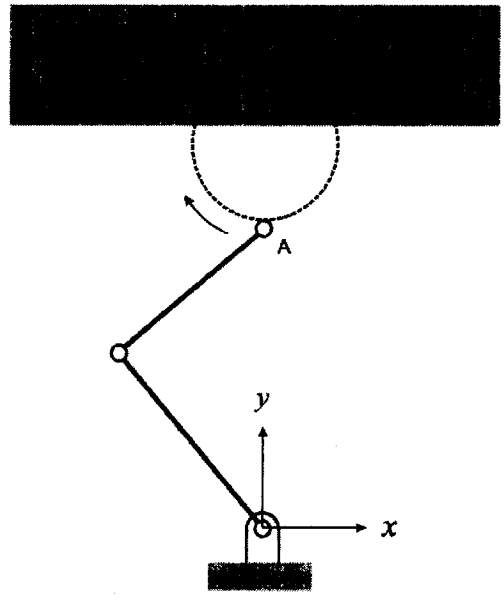

Fig. 2 Compliant contact task of a two-link manipulator interacting with an unknown environment

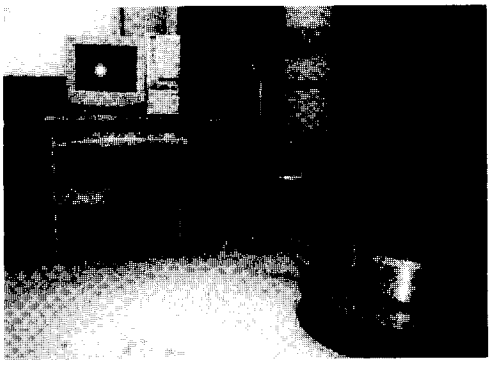

Fig. 3 Laboratory-developed two-link direct drive manipulator and its control system

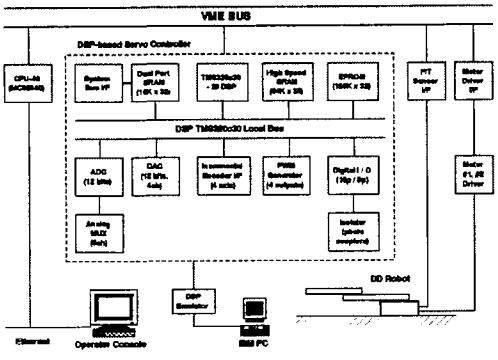

Fig. 4 The hardware configuration of the controller for a two-link manipulator

the object in which the contact forces are to be regulated. For our experimental system, the task is given as shown in Fig. 2. Specifically, the given task is to follow a circular trajectory starting from point A in the unconstrained space, to follow the wall in the constrained space, to follow the well in the constrained space, and to return to the point A. The virtual trajectory in our case is a portion of the circle as shown in Fig. 2.

For experimental verification of the proposed stiffiness control algorithm, a two-link direct drive manipulator developed in our laboratory is used as shown in Fig. 3. The joints are directly actuated by megatorque motors RS0608FN001 and RS14010FN001 manufactured by Nippon Seiko Ltd., with shaft resolvers providing motor position measurements. Joint velocities are reconstructed through numerical differentiation of the joint position measurements. A six-axis wrist

Table 1 Physical parameters of the robot manipulator

Items	*Link* 1	*Link* 2
Length (m)	0.403	0.453
Mass of Link (Kg)	22	12
Mass of motor(Kg)	73	14
Rotor inertia ($Kgfm^2$)	1.07	0.031

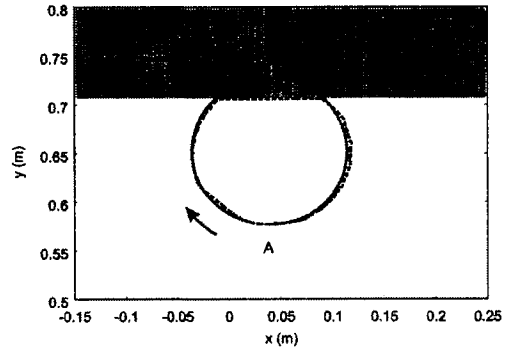

(a) Trajectory of the end-point

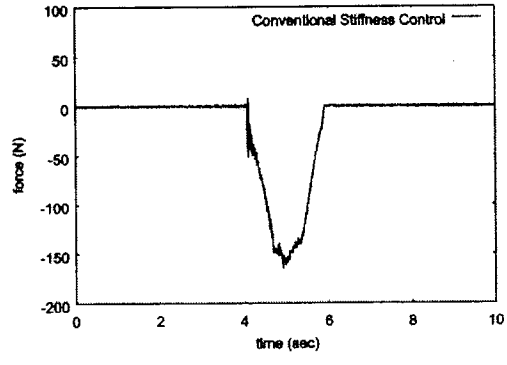

(b) The history of contact force

Fig. 5 Actual position and force trajectories in the case of the fixed stiffness gains

force/torque sensor, Model No. 67M25A-I40 of JR3 Inc., is mounted at the end-effector for measuring contact force/torque. The physical parameters of the manipulator are given in Table 1.

The robot maniplulator is controlled by a VME-bus based real-time control system shown in Fig. 4. The main control loop is provided by an in-house DSP-based servo controller. The contact force signal of the end-effector is obtained by a force/torque interface board after the noise has been filtered, and then the force information

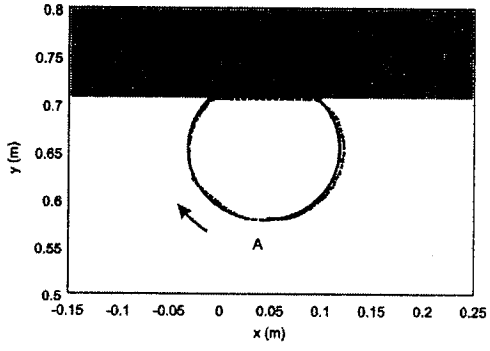

(a) Trajectory of the end-point

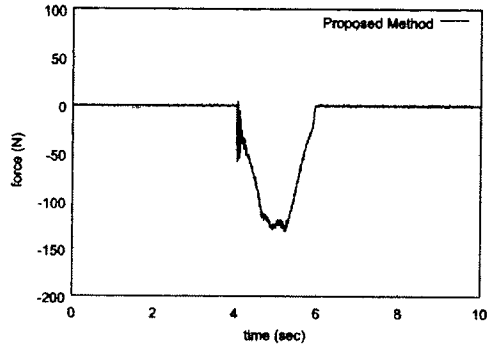

(b) The history of contact force

Fig. 6 Actual position and force trajectories when adaptive stiffness law is used ($s_x=s_y=0.005$)

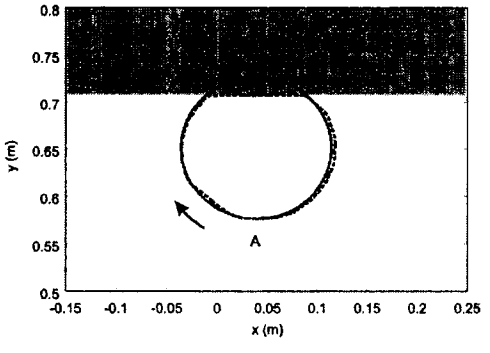

(a) Trajectory of the end-point

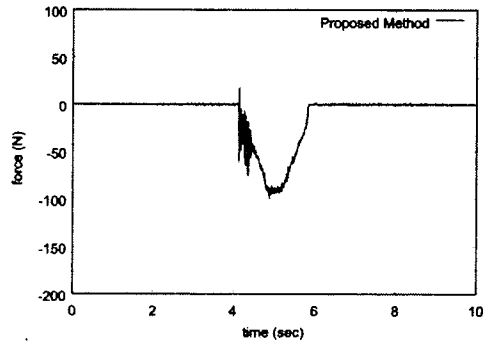

(b) The history of contact force

Fig. 7 Actual position and force trajectories when adaptive stiffness law is used ($s_x=s_y=0.015$)

is transmitted to the DSP controller and the single board computer MC68040 through the VME-bus. The analog signals are sampled and digitized by the A/D converter, and the torque commands are transferred to each actuator by the D/A converter. The current joint position of the robot manipulator is measured from the resolver signal processing units at every sampling time of 5 msec. The control algorithms are coded in a C language. The control signal update and the data feedback for each joint are executed at every sampling time with the aid of the real-time O. S. VxWorks(VxWorks Manual, 1992).

3.2 Experimental results

To test the effectiveness of the proposed stiffness control algorithm, a simple task is chosen as shown in Fig. 2. In the experiments, we give a diameter of circle as 0.15 m and task time to be 10 secs. The stiffness gains K_{cx} and K_{cy} are initially selected to be 4265.0, and the scaling parameters, α_x and α_y, are set at 0.01.

The experimental results are shown in Figs. 5, 6, and 7. For both the constant stiffness gains of Fig. 5 and the proposed force error based adaptive stiffness functions of Figs. 6 and 7, the system shows stable operations through all phases of the task. In particular, similar path following performances are obtained. However, the interaction forces during the constrained motion phase of the task are shown to be quite different. In Fig. 5, one can observe that if the constant stiffiness control is used, the interaction force increases rapidly as the position error and hence the reaction force increases. However, Figs. 6 and 7 show that the maximum reaction forces have decreased by about 19% and 38%, respectively.

These two figures show that by applying the proposed contol algorithm, the reaction force can be significantly reduced. Moreover, the extent of the reduction is influenced by the choice of the slope parameters, as shown in Figs. 6 and 7. The

slope parameters should be carefully chosen as it causes the bouncing effect during the transition stage from the unconstrained space to the constrained space.

4. Concluding Remarks

A new compliant control strategy that employs a self-controlled stiffness function was proposed in this paper. The proposed scheme is very useful for controlling various types of manipulator motions such as path following, initial contact with soft impact and force regulation during contact and does not require any switching algorithm nor any knowledge of the environment in the constrained and unconstrained spaces. The proposed method was experimentally shown to work satisfactorily for a compliance control task by a laboratory-developed two-link manipulator.

References

Chiaverini, S., Sicilliano, B., and Villani, L., 1998, "Force and Position Tracking : Parallel Control With Stiffness Adaptation," *IEEE Control Systems Magazine,* Vol. 18, No. 1, pp. 27 ~33.

Kang, S., Kim, M., and Lee, K. -I., 1998, "Assembly of Complex Shaped Objects : A Stiffness Control with Contact Localization," *KSME Int. Journal,* Vol. 12, No. 3, pp. 451~460.

Kim, K. I., 1999, "Two Strategis for Handling Unknown Loads of Two Coordinating Robots," *KSME Int. Journal,* Vol. 13, No. 2, pp. 116~129.

Lewis, F. L., Abdallah, C. T., and Dawson, D. M., 1993, *Control of Robot Manipulators,* Macmillan Publishing Company.

Oh, S. -R., Kim H. C., Suh, I. H., You, B. -J., and Lee, C. -W., 1995, "A Compliance Control Strategy for Robot Manipulators Using a Self-Controlled Stiffness Function," *Proc. of IEEE/RSJ Int. Conf. Intelligent Robots and Systems,* pp. 179~184.

Raibert, M. H. and Craig, J. J., 1981, "Hybrid Position/Force Control of Manipulators," *ASME J. Dyn. Syst. Meas. Contr.,* Vol. 102, No. 1, pp. 126~133.

Salisbury, J. K., 1980, "Active Stiffness Control of Manipulator in Cartesian Coordinates," *Proc. of IEEE 19th Conf. on Decision and Control,* pp. 95~100.

Schutter, J. De and Brussel, H. Van, 1988, "Compliant Robot Motion II. A Control Approach Based on External Control Loops," *Int. J. of Robotics Research,* Vol. 7, No. 4, pp. 18 ~143.

Vukobratović, M., and Tuneski, A., 1994, "Contact Control Concepts in Manipulation Robotics-An Overview," *IEEE Trans. on Industr. Electro.,* Vol, 41, No. 1, pp. 12~24.

VxWorks Manual, 1992, *Real-Time Operating System,* Wind River Systems.

Yoshikawa, T., 1987, "Dynamic Hybrid Position/Force Control of Robot Manipulators-Description of Hand Constraints and Calculation of Joint Driving Force," *IEEE J. of Robotics and Automation,* Vol. 33, pp. 386~392.